Letter

Optimal linear cyclic quantum heat engines cannot benefit from strong coupling

Junjie Liu [1,*] and Kenneth A. Jung [2,†]

[1] *Department of Physics, International Center of Quantum and Molecular Structures, Shanghai University, Shanghai 200444, China*

[2] *Department of Chemistry, Stanford University, Stanford, California 94305, USA*

(Received 8 June 2022; revised 5 July 2022; accepted 15 August 2022; published 30 August 2022)

Uncovering whether strong system-bath coupling can be an advantageous operation resource for energy conversion can facilitate the development of efficient quantum heat engines (QHEs). Yet, a consensus on this ongoing debate is still lacking owing to challenges arising from treating strong couplings. Here, we conclude the debate for optimal linear cyclic QHEs operated under a small temperature difference by revealing the detrimental role of strong system-bath coupling in their optimal operations. We analytically demonstrate that both the efficiency at maximum power and maximum efficiency of strong-coupling linear cyclic QHEs are upper bounded by their weak-coupling counterparts with the same degree of time-reversal symmetry breaking. Under strong time-reversal symmetry breaking, we further reveal a quadratic suppression of the optimal efficiencies relative to the Carnot limit when away from the weak-coupling regime, along with a quadratic enhancement of the mean entropy production rate.

DOI: 10.1103/PhysRevE.106.L022105

Introduction. The miniaturization of controllable quantum systems opens doors for realizing nanoscale quantum heat engines (QHEs) that enable heat-work conversion in the quantum realm [1–10]. At the nanoscale, the surface area of the working substances of QHEs could easily become comparable to their volume [1,4,6,7,10–13], which gives rise to scenarios where the strong system-bath coupling limit is attainable [6]. Investigating such strong-coupling QHEs requires a quantum thermodynamic framework that extends beyond the classical version where system-bath coupling is assumed to be negligible [14]. Hence strong-coupling QHEs can serve as a vital platform for demonstrating intrinsic quantum signatures of energy conversion [7,15,16]. Moreover, analyzing the performance of strong-coupling QHEs allows for validation of proposed definitions for thermodynamic quantities at strong couplings [17,18], an ongoing topic of strong-coupling thermodynamics (see a recent review [19] and references therein).

Understanding the role of system-bath coupling in heat-work conversion can advance the field of strong-coupling QHEs. Substantial efforts have been put into the investigation of whether strong system-bath coupling can lead to operation advantages. To date, no general consensus has yet been reached, in part due to theoretical and numerical challenges imposed by strong system-bath couplings [19]. In this ongoing debate there are studies that claim system-bath coupling could be a useful resource which potentially enhances the performance of QHEs [20–25] and there are results suggesting detrimental effects of finite system-bath coupling [26–32]. This lack of agreement stems from the fact that existing studies on strong-coupling QHEs are largely carried out on either specific models [20,21,25,27–30] or specific cycles [22–24,26,31,32] which limits the generality of their conclusions on the role of system-bath coupling in heat-work conversion.

Here, we focus on *generic* periodically driven QHEs from weak to strong couplings operated in the linear-response regime characterized by a small temperature difference (we will refer to these as linear cyclic QHEs hereafter). Using a complete form of the first law of thermodynamics which holds for generic cyclic QHEs [23] and leveraging the principals of linear irreversible thermodynamics [33], we reveal a *universal* feature of linear cyclic QHEs that *optimal* weak-coupling machines perform more efficiently than their strong-coupling counterparts with the same degree of time-reversal symmetry breaking, conditional only on the non-negativity of both the entropy production rate and the efficiency of QHEs. We gain this general insight by first obtaining thermodynamic bounds on the efficiency at maximum power and maximum efficiency [cf. Eqs. (16) and (19)] of linear cyclic QHEs valid from weak to strong couplings, then demonstrating that both the efficiency at maximum power and maximum efficiency of linear cyclic QHEs are upper bounded by their weak-coupling limits [cf. Eqs. (17) and (20)]. Our thermodynamic bounds on optimal figures of merit reduce to known forms [34,35] in the weak-coupling limit, thereby indicating that the existing thermodynamic bounds [34,35] when applying to cyclic QHEs are only applicable at weak couplings [36,37]. We also find that both the efficiency at maximum power and maximum efficiency of strong-coupling linear cyclic QHEs are quadratically suppressed from the Carnot limit under strong time-reversal symmetry breaking [cf. Eqs. (17) and (20)]. Interestingly, we can attribute this quadratic suppression of optimal efficiencies to a quadratic enhancement of the mean entropy production rate in the same limit [cf. Eq. (22)]. Our findings uncover a universal detrimental role of strong system-bath coupling in shaping the optimal performance of generic

*jj_liu@shu.edu.cn

†kajung@stanford.edu

linear cyclic QHEs, and provide crucial insight into the search of efficient strong-coupling QHEs over weak-coupling counterparts as one steps out of the linear-response regime.

Linear cyclic QHEs. We consider generic cyclic QHEs as described by the total Hamiltonian ($\hbar = 1$ and $k_B = 1$ hereafter)

$$H(t) = H_S(t) + H_I(t) + H_B. \tag{1}$$

Here, $H_S(t)$ describes a periodically driven working substance, and $H_B = \sum_{v=h,c} H_B^v$ includes a hot (h) and a cold (c) heat bath at temperatures T_v. $H_I(t) = \sum_v H_I^v(t)$ denotes a time-dependent system-bath coupling allowing for the implementation of thermodynamic strokes. We take periodic protocols such that $H_{S,I}(\mathcal{T}) = H_{S,I}(0)$ with $\mathcal{T}$ being the period of the cycle. We assume that the cyclic QHE has reached its time-periodic limit cycle at $t = 0$, after a transient warming-up operation stage [23].

For strong-coupling cyclic QHEs in the limit-cycle phase, it was recently emphasized that the first law of thermodynamics should take the following complete form [23],

$$J_W + \sum_v J_{Q_v} - J_A = 0. \tag{2}$$

Here, $J_{W,Q_v,A}$ are cycle-averaged thermodynamic fluxes [36–39] corresponding to the work, heat, and system-bath coupling ($\alpha = W, Q_v, A$),

$$J_\alpha \equiv \frac{1}{\mathcal{T}} \int_0^{\mathcal{T}} dt\, d_t \langle \mathcal{O}_\alpha \rangle, \tag{3}$$

where $\mathcal{O}_W = H(t)$, $\mathcal{O}_{Q_v} = -H_B^v$, and $\mathcal{O}_A = H_I(t)$, respectively, noting $\int_0^{\mathcal{T}} dt\, d_t \langle H_S(t) \rangle = 0$ at the limit cycle. $\langle \mathcal{O} \rangle \equiv \mathrm{Tr}[\rho(t)\mathcal{O}]$ denotes an ensemble average of any observable $\mathcal{O}$ over the global density matrix $\rho(t)$ of the composite system $H(t)$, $d_t \mathcal{O} \equiv d\mathcal{O}/dt$. In our convention, a heat engine mode corresponds to $J_W < 0$, $J_{Q_h} > 0$, and $J_{Q_c} < 0$. We point out that J_W encompasses work contributions from both driving the working medium and tuning on/off the interaction [40] since $d_t \langle H(t) \rangle = \langle d_t H(t) \rangle$ and $J_A \cdot \mathcal{T}$ accounts for the energy accumulated in the interaction term over a limit cycle. We focus on typical setups with $[H_I, H_S + H_B] \neq 0$ such that J_A vanishes only at weak couplings in the limit-cycle phase [23]. The mean entropy production rate σ over a limit cycle is given by

$$\sigma = -\sum_v \beta_v J_Q^v. \tag{4}$$

Here, $\beta_v = 1/T_v$ are the inverse temperatures of heat baths.

We consider a small temperature difference $\Delta T/T_v \ll 1$ with $\Delta T = T_h - T_c$, thereby allowing for a linear-response description of cyclic QHEs. Combining Eqs. (2) and (4), we find $\sigma = \beta_c(J_W - J_A) + (\beta_c - \beta_h)J_Q^h$ which motivates us to introduce thermodynamic affinities $\mathcal{F}_W = \beta_c$ and $\mathcal{F}_Q = \beta_c - \beta_h > 0$ together with a renormalized work flux $J_{\widetilde{W}} \equiv J_W - J_A$ and a heat flux $J_Q \equiv J_{Q_h}$. We remark that by introducing a renormalized work flux we aim to develop a linear-response description that naturally incorporates as a special limit the existing version for cyclic QHEs at weak couplings (see, e.g., Refs. [36,37]) where J_A vanishes.

Within linear irreversible thermodynamics [33], we can write down equations relating fluxes and affinities,

$$\begin{aligned} J_{\widetilde{W}} &= L_{\widetilde{W}\widetilde{W}}\mathcal{F}_W + L_{\widetilde{W}Q}\mathcal{F}_Q, \\ J_Q &= L_{Q\widetilde{W}}\mathcal{F}_W + L_{QQ}\mathcal{F}_Q. \end{aligned} \tag{5}$$

The kinetic coefficients $L_{\alpha\beta}$ ($\alpha, \beta = \widetilde{W}, Q$) introduced above can be cast into the so-called Onsager matrix

$$\mathbb{L} = \begin{pmatrix} L_{\widetilde{W}\widetilde{W}} & L_{\widetilde{W}Q} \\ L_{Q\widetilde{W}} & L_{QQ} \end{pmatrix}. \tag{6}$$

We now find $\sigma = \sum_{\alpha,\beta} L_{\alpha\beta}\mathcal{F}_\alpha\mathcal{F}_\beta = \frac{\boldsymbol{\mathcal{F}}^T(\mathbb{L}+\mathbb{L}^T)\boldsymbol{\mathcal{F}}}{2} \equiv \boldsymbol{\mathcal{F}}^T\mathbb{L}^s\boldsymbol{\mathcal{F}}$ with $\boldsymbol{\mathcal{F}} = (\mathcal{F}_W, \mathcal{F}_Q)^T$ a 2×1 vector and $\mathbb{L}^s \equiv (\mathbb{L} + \mathbb{L}^T)/2$ being the symmetric part of the matrix $\mathbb{L}$; the superscript T denotes the transpose. The non-negativity of σ thus indicates that the symmetric part $\mathbb{L}^s$ must be positive semidefinite [37], leading to the following constraints on kinetic coefficients,

$$\begin{aligned} &L_{\widetilde{W}\widetilde{W}} \geqslant 0, \quad L_{QQ} \geqslant 0, \\ &L_{\widetilde{W}\widetilde{W}}L_{QQ} - \tfrac{1}{4}(L_{\widetilde{W}Q} + L_{Q\widetilde{W}})^2 \geqslant 0. \end{aligned} \tag{7}$$

Though mathematically straightforward, the above linear-response description is not directly applicable for the characterization of the performance of strong-coupling cyclic QHEs, noting that only part of $J_{\widetilde{W}}$ corresponds to the actual work flux. We circumvent this issue by further adopting the following separations for kinetic coefficients as can be inferred from the form $J_{\widetilde{W}} = J_W - J_A$ and the linear nature of Eq. (5) [41], $L_{\widetilde{W}\widetilde{W}} = L_{WW} - L_{WA} + L_{AA} - L_{AW}$, $L_{\widetilde{W}Q} = L_{WQ} - L_{AQ}$, and $L_{Q\widetilde{W}} = L_{QW} - L_{QA}$, yielding

$$\begin{aligned} J_W &= (L_{WW} - L_{WA})\mathcal{F}_W + L_{WQ}\mathcal{F}_Q, \\ J_Q &= (L_{QW} - L_{QA})\mathcal{F}_W + L_{QQ}\mathcal{F}_Q. \end{aligned} \tag{8}$$

At weak couplings, we should have $L_{\alpha A} = L_{A\alpha} = 0$ since $J_A = (L_{AW} - L_{AA})\mathcal{F}_W + L_{AQ}\mathcal{F}_Q = 0$, where both $\mathcal{F}_W$ and $\mathcal{F}_Q$ are generally nonzero, reducing Eq. (8) to those for weak-coupling scenarios [36,37].

To facilitate an analytical treatment, one can introduce dimensionless parameters as combinations of kinetic coefficients [34]. For strong-coupling linear cyclic QHEs, we find the following four dimensionless parameters are adequate to describe thermodynamics and characterize optimal performance,

$$\begin{aligned} x &\equiv \frac{L_{WQ}}{L_{QW} - L_{QA}}, \quad y \equiv \frac{\mathcal{D}}{L_{QQ}(L_{WW} - L_{WA}) - \mathcal{D}}, \\ z_1 &\equiv \frac{L_{WQ}}{L_{WQ} - L_{AQ}}, \quad z_2 \equiv \frac{\mathcal{D}}{L_{QQ}(L_{AA} - L_{AW}) + \mathcal{D}}. \end{aligned} \tag{9}$$

Here, $\mathcal{D} \equiv (L_{WQ} - L_{AQ})(L_{QW} - L_{QA})$. At weak couplings, expressions for x and y reduce to their well-adopted forms in systems with just work and heat fluxes [34,36,37] and $z_{1,2}$ become unity. The presence of two extra parameters $z_{1,2} \neq 1$ thus distinguishes strong-coupling cyclic QHEs from weak-coupling counterparts in the linear-response regime. The ratio x/z_1 characterizes the degree of time-reversal symmetry breaking at strong couplings which is analogous to the weak-coupling scenario where x is used [36,37].

In terms of x, y, z_1, z_2 and using separations of kinetic coefficients introduced above, the constraints in Eq. (7) transfer

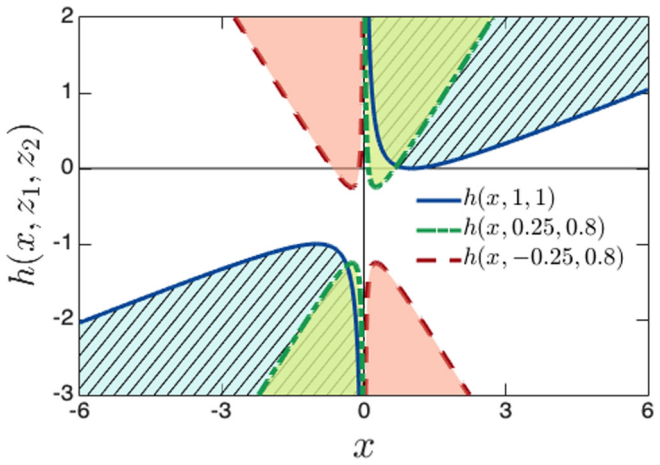

FIG. 1. Bound $h(x,z_1,z_2)$ [cf. Eq. (11)] as a function of x with $z_{1,2}=1$ (blue solid line, corresponding to the weak-coupling limit), $z_1=0.25$, $z_2=0.8$ (green dashed-dotted line), and $z_1=-0.25$, $z_2=0.8$ (red dashed line). y^{-1} can take values only from the shaded and hatched regions enclosed by $h(x,z_1,z_2)$.

to

$$\frac{1}{xz_1}\left(\frac{1}{y}+\frac{1}{z_2}\right)-\frac{1}{4}\left(\frac{1}{x}+\frac{1}{z_1}\right)^2\geqslant 0, \tag{10}$$

which yields

$$\begin{aligned} y^{-1}&\geqslant h(x,z_1,z_2), \quad \text{for } xz_1\geqslant 0,\\ y^{-1}&\leqslant h(x,z_1,z_2), \quad \text{for } xz_1<0. \end{aligned} \tag{11}$$

Here, we have introduced $h(x,z_1,z_2)\equiv[z_2(x+z_1)^2-4xz_1]/(4xz_1z_2)$. At weak couplings with $z_{1,2}=1$, the above inequalities reduce to known constraints on y: $0\leqslant y\leqslant 4x/(x-1)^2$ $[4x/(x-1)^2\leqslant y\leqslant 0]$ for $x\geqslant 0$ $(x<0)$ [34,36,37]. It can be verified that $h(x,z_1,z_2)\geqslant(z_2-1)/z_2$ $(\leqslant -1/z_2)$ in the region of $xz_1\geqslant 0$ $(xz_1<0)$. Furthermore, we note that $h(-x,-z_1,z_2)=h(x,z_1,z_2)$ which leaves the bounds in Eq. (11) unchanged. In Fig. 1, we depict a set of results for $h(x,z_1,z_2)$ with varying $z_{1,2}$ which clearly verifies the aforementioned features of $h(x,z_1,z_2)$. By contrasting the blue hatched and green shaded regions depicted in Fig. 1, one can observe that the allowed parameter region of y^{-1} shrinks and moves downwards when $z_{1,2}$ deviate from the weak-coupling limit. Particularly, y can take negative values in the region of $xz_1\geqslant 0$ when $z_{1,2}\neq 1$, in direct contrast to the weak-coupling limit where y is non-negative in the region of $x\geqslant 0$. As will be seen later, the changes in $h(x,z_1,z_2)$ lead to profound consequences on thermodynamic bounds on optimal efficiencies of linear cyclic QHEs.

Optimized performance. Using Eq. (8), the output power $P\equiv -T_c\mathcal{F}_W J_W$ and thermodynamic efficiency $\eta\equiv P/J_Q$ in the linear-response regime are given by

$$P=-T_c\mathcal{F}_W[(L_{WW}-L_{WA})\mathcal{F}_W+L_{WQ}\mathcal{F}_Q], \tag{12}$$

$$\eta=-\frac{T_c\mathcal{F}_W[(L_{WW}-L_{WA})\mathcal{F}_W+L_{WQ}\mathcal{F}_Q]}{(L_{QW}-L_{QA})\mathcal{F}_W+L_{QQ}\mathcal{F}_Q}. \tag{13}$$

We consider efficiency at maximum power (EMP) and maximum efficiency (ME) as figures of merit characterizing the optimal performance of linear cyclic QHEs from weak to strong couplings. Particularly, we are interested in general thermodynamic bounds on both the EMP and ME. To ensure the existence of *non-negative* EMP and ME for linear cyclic QHEs with y satisfying Eq. (11), we find that one should limit the ranges of $z_{1,2}$ to (see details in Supplemental Material [42])

$$0\leqslant z_1\leqslant 1, \quad \frac{1}{2-z_1}\leqslant z_2\leqslant 1. \tag{14}$$

We require that one can take $z_2=1$ only when $z_1=1$ and vice versa. Equation (14) is a direct result of the non-negativity of both the entropy production rate and optimal efficiencies, and no extra assumptions are invoked besides limiting z_1 to a positive number due to $h(-x,-z_1,z_2)=h(x,z_1,z_2)$. In the Supplemental Material [42], we address the scenario with a negative z_1 and show that the results and conclusions obtained below remain unaltered.

We first focus on the EMP and its thermodynamic bound. By maximizing the output power [cf. Eq. (12)] with respect to $\mathcal{F}_W$ [43], we receive an optimal condition $\mathcal{F}_W^o=-L_{WQ}\mathcal{F}_Q/[2(L_{WW}-L_{WA})]$. Then we can obtain the EMP $\eta(P_{\max})=P/J_Q|_{\mathcal{F}_W=\mathcal{F}_W^o}$ as

$$\eta(P_{\max})=\frac{\eta_c}{2}\frac{xyz_1}{2(1+y)-yz_1}. \tag{15}$$

Here, $\eta_c=1-T_c/T_h$ denotes the Carnot limit. In arriving at the above equation, we have used the replacement $[L_{QQ}(L_{WW}-L_{WA})]/L_{WQ}^2=(y^{-1}+1)/(xz_1)$. When $z_1=1$, we recover the known expression for $\eta(P_{\max})$ [34,36].

Since $\eta(P_{\max})$ is a decreasing (an increasing) function of y^{-1} when $xz_1\geqslant 0$ $(xz_1<0)$, $\eta(P_{\max})$ attains its maximum when $y^{-1}=h(x,z_1,z_2)$, yielding a thermodynamic upper bound $\eta_{\rm EMP}$ on the EMP $[\eta(P_{\max})\leqslant\eta_{\rm EMP}]$,

$$\eta_{\rm EMP}(x',z_{1,2})\equiv\frac{x'^2z_1^2z_2\eta_c}{z_2(x'+1)^2+2x'(2z_2-2-z_1z_2)}. \tag{16}$$

Here, we have set $x'=x/z_1$. At weak couplings where $z_{1,2}=1$, $\eta_{\rm EMP}^{\rm weak}(x)=\eta_c x^2/(x^2+1)$ which is the known bound on EMP obtained previously [34,36]. Away from the weak-coupling limit, $\eta_{\rm EMP}$ is in general not a symmetric function of x. From Eq. (16), we can deduce the following properties of $\eta_{\rm EMP}$,

$$\eta_{\rm EMP}^{\infty}=z_1^2\eta_c, \quad \text{and} \quad \eta_{\rm EMP}(x',z_{1,2})\leqslant\eta_{\rm EMP}^{\rm weak}(x'). \tag{17}$$

Here, $\eta_{\rm EMP}^{\infty}\equiv\lim_{|x'|\to\infty}\eta_{\rm EMP}$, noting $|x'|\to\infty$ corresponds to a rather strong time-reversal symmetry breaking. The proof of the inequality in Eq. (17) can be found in the Supplemental Material [42]. We remark that here we compared the $\eta_{\rm EMP}$ with the same degree of time-reversal symmetry breaking $x'=x/z_1$ which enables a fair comparison between weak-coupling and strong-coupling linear cyclic QHEs, similar for Eq. (20) below. Equation (17) represents our first main result. A typical set of results for $\eta_{\rm EMP}$ as a function of x/z_1 with varying $z_{1,2}$ satisfying Eq. (14) is depicted in Fig. 2(a). From Fig. 2(a), it is apparent that $\eta_{\rm EMP}$ remains smaller than its weak-coupling limit with $z_{1,2}=1$, and saturates $z_1^2\eta_c$ when $|x'|\to\infty$.

We then turn to the ME and its thermodynamic bound. To get the ME $\eta_{\max}$, we directly optimize Eq. (13) with respect

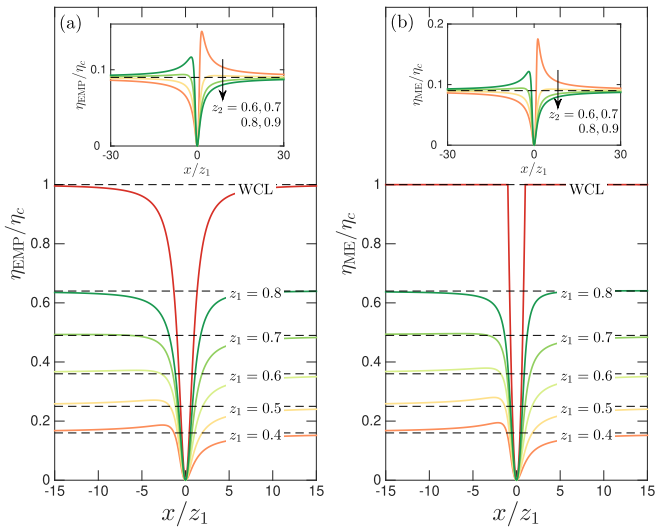

FIG. 2. (a) $\eta_{\rm EMP}/\eta_c$ [cf. Eq. (16)] as a function of x/z_1 with varying z_1 and fixed $z_2 = 0.9$. Inset: Results with varying z_2 and fixed $z_1 = 0.3$. (b) $\eta_{\rm ME}/\eta_c$ [cf. Eq. (19)] as a function of x/z_1 with varying z_1 and fixed $z_2 = 0.9$. Inset: Results with varying z_2 and fixed $z_1 = 0.3$. For comparisons, we depict the weak-coupling limit (WCL) with $z_{1,2} = 1$. Dashed horizontal lines in both plots mark the value of z_1^2.

to $\mathcal{F}_W$. After some lengthy algebra, we find (see details in Supplemental Material [42])

$$\eta_{\max} = \eta_c \frac{|x|}{|z_1 y|}(\sqrt{|1+y|} - \sqrt{|1+y-z_1 y|})^2. \tag{18}$$

Here, $|\mathcal{O}|$ takes the absolute value of $\mathcal{O}$. When $z_1 = 1$, we get $\eta_{\max} = \eta_c \frac{x}{y}(\sqrt{y+1}-1)^2 = \eta_c x \frac{\sqrt{y+1}-1}{\sqrt{y+1}+1}$ by noting $y \geqslant -1$ and x, y have the same sign, recovering the expression for $\eta_{\max}$ used in the weak-coupling limit [34,36,37]. It can be easily verified that $\eta_{\max}$ is a decreasing (an increasing) function of y^{-1} when $xz_1 \geqslant 0$ ($xz_1 < 0$). Hence, similar to the EMP, we can obtain a thermodynamic upper bound $\eta_{\rm ME}$ on the ME by taking $y^{-1} = h(x, z_1, z_2)$ in Eq. (18) ($\eta_{\max} \leqslant \eta_{\rm ME}$):

$$\eta_{\rm ME}(x', z_{1,2}) \equiv \eta_c |x'|[\sqrt{|h'+1|} - \sqrt{|(h'+1)-z_1|}]^2. \tag{19}$$

Here, we have defined $h' \equiv h(x', z_{1,2}) = [z_2(x'+1)^2 - 4x']/(4x' z_2)$. It reduces to the known bound $\eta_{\rm ME}^{\rm weak}(x) = \eta_c x^2$ (η_c) for $|x| \leqslant 1$ ($|x| \geqslant 1$) [34] when $z_{1,2} = 1$. From the above bound, we find that

$$\eta_{\rm ME}^{\infty} = z_1^2 \eta_c, \quad \text{and} \quad \eta_{\rm ME}(x', z_{1,2}) \leqslant \eta_{\rm ME}^{\rm weak}(x'). \tag{20}$$

Here, $\eta_{\rm ME}^{\infty} \equiv \lim_{|x'|\to\infty} \eta_{\rm ME}$. The proof of the inequality in Eq. (20) can be found in the Supplemental Material [42]. Equation (20) is our second main result. A typical set of results for $\eta_{\rm ME}$ as a function of x/z_1 with varying $z_{1,2}$ satisfying Eq. (14) is presented in Fig. 2(b) which clearly validates the properties listed in Eq. (20).

Combining Eqs. (17) and (20), we can draw the following general conclusions concerning the role of system-bath coupling in shaping the optimal performance of linear cyclic QHEs ($n = {\rm EMP, ME}$): Most significantly, (i) η_n is upper bounded by its weak-coupling limit, implying that an *optimal* weak-coupling cyclic QHE performs more efficiently than its strong-coupling counterpart in the linear-response regime. (ii) Noting the fact in (i) and that η_n of weak-coupling linear cyclic QHEs attains its maximum η_c under strong time-reversal symmetry breaking as $|x| \to \infty$, one can infer that optimal linear cyclic QHEs can reach the Carnot limit η_c only in the weak-coupling limit. (iii) Away from the weak-coupling limit as z_1 decreases from 1, the extreme value $\eta_n^{\infty} = z_1^2 \eta_c$ of η_n drops quadratically in z_1 relative to the Carnot limit. We can further relate z_1 to the dimensionless system-bath coupling strength λ: Denoting $H_I = \lambda \tilde{H}_I$ with $\tilde{H}_I$ a rescaled system-bath interaction, we have $J_A \propto \lambda$ by noting the definition Eq. (3) and hence $L_{\alpha A}, L_{A\alpha} \propto \lambda$ since the affinities are λ independent, leading to $z_1 \simeq 1 - c_1\lambda + \mathcal{O}(\lambda^2)$ with c_1 a model-dependent coefficient [noting the definition in Eq. (9)]. Therefore, we expect a relative suppression $(\eta_n^{\infty,\rm weak} - \eta_n^{\infty})/\eta_n^{\infty,\rm weak} = 1 - z_1^2 \propto \lambda + \mathcal{O}(\lambda^2)$ scales at least linearly in λ with $\eta_n^{\infty,\rm weak} = \eta_c$ for weak-coupling linear cyclic QHEs. We emphasize that the aforementioned conclusions hold regardless of the details of cyclic QHEs [i.e., the detailed form of $H(t)$ in Eq. (1)] provided the temperature difference between the baths is small and J_A is nonzero at strong couplings.

To gain more insight into the suppression of optimal efficiencies in the strong-coupling regime, we look at the mean entropy production rate at efficiency at maximum power $\sigma_{\rm EMP}$ and at maximum efficiency $\sigma_{\rm ME}$. We find that both $\sigma_{\rm EMP}$ and $\sigma_{\rm ME}$ have the form ($n = {\rm EMP, ME}$)

$$\sigma_n(x', z_{1,2}) = \frac{\mathcal{F}_Q^2 L_{WQ}^2}{L_{\tilde{W}\tilde{W}}} \mathcal{K}_n(x', z_{1,2}). \tag{21}$$

For simplicity, we relegate detailed functional forms of $\mathcal{K}_n(x', z_{1,2})$ to the Supplemental Material [42]; We have checked that $\mathcal{K}_n(x', z_{1,2})$ remains non-negative for $z_{1,2}$ satisfying Eq. (14). Unlike η_n, it is noticeable that σ_n contains a non-negative prefactor $\frac{\mathcal{F}_Q^2 L_{WQ}^2}{L_{\tilde{W}\tilde{W}}}$ which cannot be expressed in terms of $x', z_{1,2}$ as first noted by Ref. [34]. From the above equation, we find the weak-coupling limits: $\sigma_{\rm EMP}^{\rm weak}(x) = \frac{\mathcal{F}_Q^2 L_{WQ}^2}{L_{WW}} \frac{1}{4x^2}$ and $\sigma_{\rm ME}^{\rm weak}(x) = \frac{\mathcal{F}_Q^2 L_{WQ}^2}{L_{WW}} \frac{(x^2-1)^2}{4x^2}$ when $|x| \leqslant 1$ (and vanishes otherwise) [42]. The latter was first obtained by Ref. [34]. We highlight that it is inappropriate to contrast σ_n and $\sigma_n^{\rm weak}$ directly due to the presence of nonequal prefactors. Nevertheless, we can still analyze the asymptotic behavior of σ_n in the limit of $|x'| \to \infty$. Since one can carry out linear-response theory in that limit, it is reasonable to assume that kinetic coefficients remain finite when varying x'. We find that [42]

$$\sigma_n^{\infty} = \frac{1}{4}\left(\frac{1}{z_1} - 1\right)^2 \frac{\mathcal{F}_Q^2 L_{WQ}^{\infty,2}}{L_{\tilde{W}\tilde{W}}^{\infty}}. \tag{22}$$

Here, $\sigma_n^{\infty} \equiv \lim_{|x'|\to\infty} \sigma_n(x', z_{1,2})$ and $L_{\alpha\beta}^{\infty} = \lim_{|x'|\to\infty} L_{\alpha\beta}$. Interestingly, when z_1 decreases from 1, σ_n^{∞} experiences a quadratic enhancement compared to its vanishing weak-coupling limit (noting $\eta_n^{\infty,\rm weak} = \eta_c$). We thus attribute the quadratic suppression of η_n^{∞} relative to the Carnot limit to this quadratic enhancement of σ_n^{∞}.

Discussion. It is interesting to explore whether optimal weak-coupling cyclic QHEs can outperform their strong-coupling counterparts beyond the linear-response regime. To provide a hint, consider a reversible thermodynamic cycle

with vanishing entropy production which usually necessitates the ME. Specifically, we have $S = -\sum_v \beta_v Q_v = \beta_c(W - A) + (\beta_c - \beta_h)Q_h = 0$ ($S = \mathcal{T}\sigma$, $Q_v = \mathcal{T}J_{Q_v}$, $W = \mathcal{T}J_W$, and $A = \mathcal{T}J_A$), yielding $W = A - \eta_c Q_h$ with η_c the Carnot efficiency. Inserting the expression for W into the definition of efficiency $\eta = -W/Q_h$, we get the ME $\eta_{\max} = \eta_c - A/Q_h$. Recognizing that optimal strong-coupling cyclic QHEs with normal thermal baths cannot break the Carnot limit, we should have $A > 0$ at strong couplings by noting $Q_h > 0$; A remains nonzero at strong couplings as long as $W \neq 0$ [23], consequently, one naturally infers $\eta_{\max} \leqslant \eta_{\max}^{\text{weak}} = \eta_c$. Hence, we conjecture that strong coupling will likely suppress the ME of cyclic QHEs beyond the linear-response regime. We leave possible validations to future works.

To correctly interpret the present results, it is necessary to discriminate between optimal and nonoptimal QHEs. Taking a set of $z_{1,2} < 1$, we only stated that $\eta_n(z_{1,2}) < \eta_n^{\text{weak}} \equiv \eta_n(z_{1,2} = 1)$ with $n = \text{EMP, ME}$ in the linear-response regime. However, if one just considers a nonoptimal linear QHE with an actual efficiency $\eta < \eta_n$, it is possible to have the trend $\eta(z_{1,2}) > \eta^{\text{weak}} \equiv \eta(z_{1,2} = 1)$ as opposed to the relative relation for the optimal efficiency η_n, namely, our present results do not rule out the possibility of having nonoptimal cyclic QHEs capable of benefitting from strong couplings in the linear-response regime.

In summary, we analyzed the optimal performance of generic cyclic QHEs from weak to strong couplings in the linear-response regime and obtained thermodynamic bounds on optimal efficiencies. We revealed a universal feature of linear cyclic QHEs that system-bath coupling tends to suppress both the efficiency at maximum power and maximum efficiency. Under strong time-reversal symmetry breaking, this suppression scales at least linearly in system-bath coupling strength. Our results provide insight into the investigation of the effects of system-bath coupling on heat-work conversion and are relevant for the search of efficient strong-coupling QHEs.

Acknowledgments. We thank Dvira Segal for helpful discussions. J.L. acknowledges support from the startup funding of Shanghai University. K.A.J. acknowledges support from the National Science Foundation Grant No. CHE-2154291.

[1] O. Abah, J. Roßnagel, G. Jacob, S. Deffner, F. Schmidt-Kaler, K. Singer, and E. Lutz, Single-Ion Heat Engine at Maximum Power, Phys. Rev. Lett. **109**, 203006 (2012).

[2] J. Roßnagel, O. Abah, F. Schmidt-Kaler, K. Singer, and E. Lutz, Nanoscale Heat Engine Beyond the Carnot Limit, Phys. Rev. Lett. **112**, 030602 (2014).

[3] A. Dechant, N. Kiesel, and E. Lutz, All-Optical Nanomechanical Heat Engine, Phys. Rev. Lett. **114**, 183602 (2015).

[4] J. Roßnagel, S. T. Dawkins, K. N. Tolazzi, O. Abah, E. Lutz, F. Schmidt-Kaler, and K. Singer, A single-atom heat engine, Science **352**, 325 (2016).

[5] S. Krishnamurthy, S. Ghosh, D. Chatterji, R. Ganapathy, and A. K. Sood, A micrometre-sized heat engine operating between bacterial reservoirs, Nat. Phys. **12**, 1134 (2016).

[6] J. P. S. Peterson, T. B. Batalhão, M. Herrera, A. M. Souza, R. S. Sarthour, I. S. Oliveira, and R. M. Serra, Experimental Characterization of a Spin Quantum Heat Engine, Phys. Rev. Lett. **123**, 240601 (2019).

[7] J. Klatzow, J. N. Becker, P. M. Ledingham, C. Weinzetl, K. T. Kaczmarek, D. J. Saunders, J. Nunn, I. A. Walmsley, R. Uzdin, and E. Poem, Experimental Demonstration of Quantum Effects in the Operation of Microscopic Heat Engines, Phys. Rev. Lett. **122**, 110601 (2019).

[8] R. J. de Assis, T. M. de Mendonça, C. J. Villas-Boas, A. M. de Souza, R. S. Sarthour, I. S. Oliveira, and N. G. de Almeida, Efficiency of a Quantum Otto Heat Engine Operating Under a Reservoir at Effective Negative Temperatures, Phys. Rev. Lett. **122**, 240602 (2019).

[9] J. P. Pekola and I. M. Khaymovich, Thermodynamics in single-electron circuits and superconducting qubits, Annu. Rev. Condens. Matter Phys. **10**, 193 (2019).

[10] D. von Lindenfels, O. Gräb, C. T. Schmiegelow, V. Kaushal, J. Schulz, M. T. Mitchison, J. Goold, F. Schmidt-Kaler, and U. G. Poschinger, Spin Heat Engine Coupled to a Harmonic-Oscillator Flywheel, Phys. Rev. Lett. **123**, 080602 (2019).

[11] K. Ono, S. N. Shevchenko, T. Mori, S. Moriyama, and F. Nori, Analog of a Quantum Heat Engine Using a Single-Spin Qubit, Phys. Rev. Lett. **125**, 166802 (2020).

[12] W. Ji, Z. Chai, M. Wang, Y. Guo, X. Rong, F. Shi, C. Ren, Y. Wang, and J. Du, Spin Quantum Heat Engine Quantified By Quantum Steering, Phys. Rev. Lett. **128**, 090602 (2022).

[13] M. Josefsson, A. Svilans, A. M. Burke, E. A. Hoffmann, S. Fahlvik, C. Thelander, M. Leijnse, and H. Linke, A quantum-dot heat engine operating close to the thermodynamic efficiency limits, Nat. Nanotechnol. **13**, 920 (2018).

[14] L. A. Pachón, J. F. Triana, D. Zueco, and P. Brumer, Influence of non-Markovian dynamics in equilibrium uncertainty-relations, J. Chem. Phys. **150**, 034105 (2019).

[15] R. Uzdin, A. Levy, and R. Kosloff, Equivalence of Quantum Heat Machines, and Quantum-Thermodynamic Signatures, Phys. Rev. X **5**, 031044 (2015).

[16] R. Dann and R. Kosloff, Quantum signatures in the quantum Carnot cycle, New J. Phys. **22**, 013055 (2020).

[17] Á. Rivas, Strong Coupling Thermodynamics of Open Quantum Systems, Phys. Rev. Lett. **124**, 160601 (2020).

[18] P. Strasberg and M. Esposito, Measurability of nonequilibrium thermodynamics in terms of the Hamiltonian of mean force, Phys. Rev. E **101**, 050101(R) (2020).

[19] P. Talkner and P. Hänggi, *Colloquium:* Statistical mechanics and thermodynamics at strong coupling: Quantum and classical, Rev. Mod. Phys. **92**, 041002 (2020).

[20] D. Gelbwaser-Klimovsky and A. Aspuru-Guzik, Strongly coupled quantum heat machines, J. Phys. Chem. Lett. **6**, 3477 (2015).

[21] P. Strasberg, G. Schaller, N. Lambert, and T. Brandes, Nonequilibrium thermodynamics in the strong coupling and non-Markovian regime based on a reaction coordinate mapping, New J. Phys. **18**, 073007 (2016).

[22] Y. Y. Xu, B. Chen, and J. Liu, Achieving the classical Carnot efficiency in a strongly coupled quantum heat engine, Phys. Rev. E **97**, 022130 (2018).

[23] J. Liu, K. A. Jung, and D. Segal, Periodically Driven Quantum Thermal Machines from Warming Up to Limit Cycle, Phys. Rev. Lett. **127**, 200602 (2021).

[24] Y. Shirai, K. Hashimoto, R. Tezuka, C. Uchiyama, and N. Hatano, Non-Markovian effect on quantum Otto engine: Role of system-reservoir interaction, Phys. Rev. Research **3**, 023078 (2021).

[25] M. Carrega, L. M. Cangemi, G. De Filippis, V. Cataudella, G. Benenti, and M. Sassetti, Engineering dynamical couplings for quantum thermodynamic tasks, PRX Quantum **3**, 010323 (2022).

[26] R. Gallego, A. Riera, and J. Eisert, Thermal machines beyond the weak coupling regime, New J. Phys. **16**, 125009 (2014).

[27] A. Kato and Y. Tanimura, Quantum heat current under non-perturbative and non-Markovian conditions: Applications to heat machines, J. Chem. Phys. **145**, 224105 (2016).

[28] D. Newman, F. Mintert, and A. Nazir, Performance of a quantum heat engine at strong reservoir coupling, Phys. Rev. E **95**, 032139 (2017).

[29] S. Restrepo, J. Cerrillo, P. Strasberg, and G. Schaller, From quantum heat engines to laser cooling: Floquet theory beyond the Born–Markov approximation, New J. Phys. **20**, 053063 (2018).

[30] D. Newman, F. Mintert, and A. Nazir, Quantum limit to nonequilibrium heat-engine performance imposed by strong system-reservoir coupling, Phys. Rev. E **101**, 052129 (2020).

[31] M. Perarnau-Llobet, H. Wilming, A. Riera, R. Gallego, and J. Eisert, Strong Coupling Corrections in Quantum Thermodynamics, Phys. Rev. Lett. **120**, 120602 (2018).

[32] M. Kaneyasu and Y. Hasegawa, Strong coupling quantum Otto cycle, arXiv:2205.09400.

[33] H. B. Callen, *Thermodynamics and an Introduction to Thermostatics* (Wiley, New York, 1985).

[34] G. Benenti, K. Saito, and G. Casati, Thermodynamic Bounds on Efficiency for Systems with Broken Time-Reversal Symmetry, Phys. Rev. Lett. **106**, 230602 (2011).

[35] J.-H. Jiang, Thermodynamic bounds and general properties of optimal efficiency and power in linear responses, Phys. Rev. E **90**, 042126 (2014).

[36] K. Brandner, K. Saito, and U. Seifert, Thermodynamics of Micro- and Nano-Systems Driven by Periodic Temperature Variations, Phys. Rev. X **5**, 031019 (2015).

[37] K. Brandner and U. Seifert, Periodic thermodynamics of open quantum systems, Phys. Rev. E **93**, 062134 (2016).

[38] K. Brandner, M. Bauer, and U. Seifert, Universal Coherence-Induced Power Losses of Quantum Heat Engines in Linear Response, Phys. Rev. Lett. **119**, 170602 (2017).

[39] H. J. D. Miller, M. H. Mohammady, M. Perarnau-Llobet, and G. Guarnieri, Thermodynamic Uncertainty Relation in Slowly Driven Quantum Heat Engines, Phys. Rev. Lett. **126**, 210603 (2021).

[40] M. Wiedmann, J. Stockburger, and J. Ankerhold, Non-Markovian dynamics of a quantum heat engine: out-of-equilibrium operation and thermal coupling control, New J. Phys. **22**, 033007 (2020).

[41] Alternatively, one can obtain the same separations by first writing down linear equations connecting $J_{W,Q,A}$ and $\mathcal{F}_{W,Q,A}$; $\sigma = \sum_{\alpha=W,Q,A} \mathcal{F}_\alpha J_\alpha$, and then combining the coefficients by noting $\mathcal{F}_A \equiv -\beta_c = -\mathcal{F}_W$.

[42] See Supplemental Material at http://link.aps.org/supplemental/10.1103/PhysRevE.106.L022105 for derivation details regarding the maximum efficiency, ranges of $z_{1,2}$ enabling non-negative optimal figures of merit, the mean entropy production rate at optimal efficiencies, and the proof of the relative relation of optimal figures of merit between strong-coupling and weak-coupling cyclic quantum heat engines.

[43] This optimization corresponds to varying the temperatures of thermal baths while fixing the temperature difference.